Swiss National Science Foundation under contract 2.035–0.86.

References

Brown, I. D. (1985). *Acta Cryst.* A**41**, 399.

Chevalier, B., Cole, A., Lejay, P. & Etourneau, J. (1981). *Mater. Res. Bull.* **16**, 1067–1075.

Felner, I. & Nowik, I. (1980). *Phys. Rev. Lett.* **45**, 2128–2131.

Frémy, M. A., Gignoux, D., Moreau, J. M., Paccard, D. & Paccard, L. (1985). *J. Less-Common Met.* **106**, 251–255.

Hovestreydt, E. (1983). *J. Appl. Cryst.* **16**, 651–653.

International Tables for X-ray Crystallography (1974). Vol. IV. Birmingham: Kynoch Press. (Present distributor D. Reidel, Dordrecht.)

Johnston, D. C. & Braun, H. F. (1982). In *Superconductivity in Ternary Compounds* II, edited by M. B. Maple & Ø. Fischer. *Topics in Current Physics*, Vol. 34, pp. 11–55. Berlin: Springer.

Jung, W. (1977). *Z. Naturforsch. Teil B*, **32**, 1371–1374.

Jung, W. (1984). *J. Less-Common Met.* **97**, 253–263.

Jung, W. & Quentmeier, D. (1980). *Z. Kristallogr.* **151**, 172–174.

Ku, H. C. (1980). PhD thesis, Univ. of California at San Diego, USA.

Ku, H. C., Ma, L. J., Tai, M. F., Wang, Y. & Horng, H. E. (1985). *J. Less-Common Met.* **109**, 219–228.

Ku, H. C. & Meisner, G. P. (1981). *J. Less-Common Met.* **78**, 99–107.

Kuz'ma, Yu. B. & Bilonizhko, N. S. (1974). *Sov. Phys. Crystallogr.* **18**, 447–449.

Kuz'ma, Yu. B. & Bilonizhko, N. S. (1981). *Dopov. Akad. Nauk Ukr. RSR Ser. A*, **10**, 87–90.

Kuz'ma, Yu. B., Dub, O. M. & Chaban, N. F. (1985). *Dopov. Akad. Nauk Ukr. RSR Ser. B*, **7**, 36–39.

Kuz'ma, Yu. B., Kripyakevich, P. I. & Bilonizhko, N. S. (1969). *Dopov. Akad. Nauk Ukr. RSR Ser. A*, pp. 939–941.

Main, P., Fiske, S. J., Hull, S. E., Lessinger, L., Germain, G., Declercq, J.-P. & Woolfson, M. M. (1980). *MULTAN*80. *A System of Computer Programs for the Automatic Solution of Crystal Structures from X-ray Diffraction Data*. Univs. of York, England, and Louvain, Belgium.

Parthé, E. & Chabot, B. (1984). In *Handbook on the Physics and Chemistry of Rare Earths*, edited by K. A. Gschneidner Jr & L. Eyring, Vol. 6, Ch. 48, pp. 113–334. Amsterdam: North-Holland.

Parthé, E., Chabot, B. A. & Cenzual, K. (1985). *Chimia*, **39**, 164–174.

Rogl, P. (1980). *J. Nucl. Mater.* **92**, 292–298.

Rykhal, R. M., Zarechnyuk, O. S. & Kuten, Ya. I. (1978). *Dopov. Akad. Nauk Ukr. RSR Ser. A*, pp. 1136–1138.

Schmidt, B. & Jung, W. (1978). *Z. Naturforsch. Teil B*, **33**, 1430–1433.

Shelton, R. N. (1978). *J. Less-Common Met.* **62**, 191–196.

Stewart, J. M., Machin, P. A., Dickinson, C. W., Ammon, H. L., Heck, H. & Flack, H. (1976). The *XRAY*76 system. Tech. Rep. TR-446. Computer Science Center, Univ. of Maryland, College Park, Maryland, USA.

Teatum, E., Gschneidner, K. Jr & Waber, J. (1960). Cited in *The Crystal Chemistry and Physics of Metals and Alloys* (1972), edited by W. B. Pearson, p. 151. New York: John Wiley.

Vandenberg, J. M. & Barz, H. (1980). *Mater. Res. Bull.* **15**, 1493–1498.

Vlasse, M., Ohtani, T., Chevalier, B. & Etourneau, J. (1983). *J. Solid State Chem.* **46**, 188–192.

Voroshilov, Yu. V., Kripyakevich, P. I. & Kuz'ma, Yu. B. (1971). *Sov. Phys. Crystallogr.* **15**, 813–816.

Yarmolyuk, Ya. P. (1986). *Sov. Phys. Crystallogr.* **31**, 234–235.

Yarmolyuk, Ya. P. & Grin', Yu. N. (1979). Third Interunion Seminar for Young Scientists – Contemporary Problems in Crystal Chemistry, Tezisy Dokl., L'vov, pp. 69–70.

Zarechnyuk, O. S. & Rykhal, R. M. (1981). *Vestn. L'vovsk Univ. Ser. Khim.* **23**, 45–47.

Acta Cryst. (1988). C**44**, 226–229

Small Atomic Displacements in the Molybdenophosphates $AMo_2P_3O_{12}$ (A = K, Rb, Tl)

By André Leclaire and Bernard Raveau

Laboratoire de Cristallographie et Sciences des Matériaux, CRISMAT, UA 251, *ISMRA, Campus* II,
Bd du Maréchal Juin, 14032 *Caen CEDEX, France*

(*Received* 9 *April* 1987; *accepted* 25 *June* 1987)

Abstract. $KMo_2P_3O_{12}$, $M_r = 515{\cdot}90$, orthorhombic, $Pbnm$, $a = 17{\cdot}6398\,(14)$, $b = 9{\cdot}1761\,(4)$, $c = 12{\cdot}3000\,(8)$ Å, $V = 1990{\cdot}9\,(4)$ Å^3, $Z = 8$, $D_x = 3{\cdot}44$ Mg m^{-3}, $\lambda(\text{Mo } K\alpha) = 0{\cdot}71069$ Å, $\mu = 3{\cdot}42$ mm^{-1}, $F(000) = 1952$, $T = 294$ K, $R = 0{\cdot}028$ for 2123 reflections. $RbMo_2P_3O_{12}$, $M_r = 562{\cdot}26$, orthorhombic, $Pbcm$, $a = 8{\cdot}8314\,(8)$, $b = 9{\cdot}2368\,(7)$, $c = 12{\cdot}3051\,(9)$ Å, $V = 1003{\cdot}8\,(4)$ Å^3, $Z = 4$, $D_x = 3{\cdot}72$ Mg m^{-3}, $\lambda(\text{Mo } K\alpha) = 0{\cdot}71069$ Å, $\mu = 8{\cdot}08$ mm^{-1}, $F(000) = 1048$, $T = 294$ K, $R = 0{\cdot}044$ for 2073 reflections. The $Mo_2P_3O_{12}$ frameworks of the K, Rb and Tl compounds are almost the same. The main difference is in the position of the alkaline-earth ions in the tunnels, which induces, in the potassium compound, a superstructure along **a**. The alkaline-earth ions are slightly displaced as their size decreases in order that the A—O distances may agree with the sum of the ionic radii.

Introduction. Comparison of the behaviour of potassium, rubidium and thallium in different oxides with octahedral tunnel structures shows that these ions generally lead to the same structural type as shown, for instance, in the well known tungsten-bronze family A_xWO_3 (Magnéli, 1949*a*,*b*, 1952, 1953; Magnéli &

Blomberg, 1951). Moreover, the size of these ions does not drastically affect the host lattice of such oxides. However, differences may appear in the distribution of these ions in the tunnels which originate in their electronic structure: such phenomena were observed, for instance, in the bronzes Tl_xWO_3 and In_xWO_3 (Labbé, Goreaud, Raveau & Monier, 1978) in which Tl^+ and In^+ exhibit some stereoactivity due to their lone pair ns^2. Few results have been obtained for oxides with a tunnel structure characterized by a mixed framework built up from octahedra and tetrahedra, if one excepts the series of phosphate tungsten bronzes recently studied [see Raveau (1986) for a review] and some molybdenophosphates (Kierkegaard, 1962). In a recent study of the silicomolybdenophosphates, $AMo_3P_6Si_2O_{25}$ (A = K, Rb, Tl, Cs) (Leclaire, Monier & Raveau, 1984, 1985*b*; Leclaire, Borel, Grandin & Raveau, 1985) we observed that the univalent cations did not influence the framework, the parameters and the space groups of such compounds; the only difference which was observed deals with the fact that the B factor increases as the size of the A ion decreases. This behaviour was explained by the great rigidity of the mixed framework. Recently a new molybdenophosphate $TlMo_2P_3O_{12}$ with a tunnel structure was isolated and studied (Leclaire, Monier & Raveau, 1985*a*); some time afterwards the compounds with K and Rb were isolated. As $KMo_2P_3O_{12}$ exhibits a superstructure along **a** but $RbMo_2P_3O_{12}$ does not, we have determined the structure of these phosphates in order to compare the structural behaviour of potassium, rubidium and thallium in those compounds.

Experimental. A mixture of ammonium hydrogenphosphate $(NH_4)_2HPO_4$, potassium or rubidium carbonate and molybdenum oxide MoO_3 in the molecular ratio of 18/3/8 was first heated progressively up to 873 K in air, in order to decompose the carbonate and the ammonium hydrogenphosphate. The resulting product was then mixed with an adequate amount of metallic molybdenum, introduced into an alumina crucible and heated at 1273 K in an evacuated silicon ampoule for several days.

The cell parameters were determined by X-ray diffraction with a least-squares refinement based on 25 reflections. The space groups were deduced from a set of Weissenberg and precession photographs. The conditions of the data collection are shown in Table 1. Corrections were made for Lorentz and polarization effects but absorption was neglected. Both structures were solved using the heavy-atom method. Scattering factors and anomalous-dispersion corrections for the different atoms were taken from *International Tables for X-ray Crystallography* (1974). The three check reflections for each compound were stable throughout the data collection.

Table 1. *Details of data collection and refinement for* $KMo_2P_3O_{12}$ *and* $RbMo_2P_3O_{12}$

	$KMo_2P_3O_{12}$	$RbMo_2P_3O_{12}$
Crystal form	Black prism	Dark green needle
and size (mm)	0·168 × 0·072 × 0·048	0·192 × 0·060 × 0·048
θ_{max}(°)	44	45
Index range h	0→34	0→17
k	0→17	0→18
l	0→23	0→24
Scan type	ω–2θ	ω–θ
Scan angle (°)	1 + 0·35tanθ	1 + 0·35tanθ
Horizontal aperture (mm)	1 + tanθ	1 + tanθ
Monochromator	Graphite	Graphite
No. of unique reflections	2123	2073
No. with $I > 3\sigma(I)$	2123	2073
R	0·028	0·044
wR	0·028	0·043
S	1·340	1·286
No. of parameters refined	172	87
$(\Delta/\sigma)_{max}$	0·04	0·0002
Residual e Å^{-3}	1·7	1·8
Reference reflections	12,0,0	600
	250	150
	006	006

Table 2. *Atomic parameters and equivalent isotropic thermal parameters*

$$B_{eq} = \tfrac{4}{3}\textstyle\sum_i\sum_j\beta_{ij}\mathbf{a}_i.\mathbf{a}_j.$$

	x	y	z	B_{eq}(Å^2)
$KMo_2P_3O_{12}$				
Mo(1)	0·12134 (3)	0·02863 (11)	0·10175 (12)	0·31 (1)
Mo(2)	0·12450 (4)	0·47391 (11)	0·60141 (11)	0·31 (1)
K(1)	0·10031 (39)	0·66689 (67)	0·25	3·72 (12)
K(2)	0·08105 (32)	0·84247 (80)	0·75	3·09 (9)
P(1)	0·01489 (6)	0·74720 (45)	0·00178 (45)	0·41 (2)
P(2)	0·20556 (11)	0·35957 (26)	0·12961 (38)	0·45 (3)
P(3)	0·19862 (11)	0·12906 (26)	0·63085 (39)	0·38 (3)
O(1)	0·10472 (45)	0·02559 (130)	0·25	0·42 (15)
O(2)	0·10652 (49)	0·48839 (129)	0·75	0·55 (16)
O(3)	0·05640 (37)	−0·15278 (87)	0·08164 (71)	1·18 (12)
O(4)	0·07186 (31)	0·66286 (80)	0·56816 (67)	0·87 (10)
O(5)	0·15340 (34)	0·45462 (92)	0·43975 (94)	0·65 (10)
O(6)	0·14505 (37)	0·03630 (117)	−0·06255 (111)	1·23 (13)
O(7)	0·19308 (36)	0·19962 (84)	0·11840 (92)	0·90 (14)
O(8)	0·18794 (42)	0·29250 (91)	0·62266 (90)	1·07 (13)
O(9)	0·21839 (34)	0·59600 (96)	0·61991 (80)	0·96 (12)
O(10)	0·21117 (36)	0·11109 (103)	0·11836 (105)	1·29 (15)
O(11)	0·03343 (41)	0·16459 (119)	0·07897 (94)	1·25 (13)
O(12)	0·02990 (38)	0·35452 (109)	0·57243 (105)	1·38 (16)
O(13)	0·17997 (51)	0·40904 (135)	0·25	0·62 (14)
O(14)	0·17094 (65)	0·08079 (164)	0·75	1·33 (19)
$RbMo_2P_3O_{12}$				
Mo	0·24652 (4)	0·02802 (3)	0·10087 (2)	0·35 (1)
Rb	0·18821 (22)	0·16311 (14)	0·25	3·23 (3)
P(1)	0·02482 (18)	0·25	0	0·69 (2)
P(2)	0·40860 (14)	0·36033 (12)	0·12994 (10)	0·75 (2)
O(1)	0·21299 (61)	0·01666 (57)	0·25	1·02 (7)
O(2)	0·12278 (66)	0·14951 (54)	0·06757 (42)	1·90 (8)
O(3)	0·30063 (49)	0·04952 (43)	−0·06219 (30)	1·20 (6)
O(4)	0·38755 (52)	0·19860 (39)	0·12234 (37)	1·34 (7)
O(5)	0·42622 (45)	−0·10685 (46)	0·11402 (40)	1·52 (7)
O(6)	0·07001 (52)	0·16336 (52)	0·08040 (37)	1·56 (7)
O(7)	0·36130 (82)	0·41003 (69)	0·25	1·42 (9)

The atomic coordinates and anisotropic thermal factors were refined by full-matrix least squares on F and a linear weighting scheme $w = f(\sin\theta/\lambda)$ was adjusted by using the program *POND* (Leclaire, unpublished). The reliability factors were lowered to $R = 0·028$ and $wR = 0·028$ for $KMo_2P_3O_{12}$ and to $R = 0·044$ and $wR = 0·043$ for $RbMo_2P_3O_{12}$. The final atomic parameters of the two compounds are given in Table 2.*

Discussion. The cell parameters show that the behaviour of rubidium is identical to that of thallium, whereas the potassium compound differs from the other oxides by the superstructure reflections. The host lattice $[Mo_2P_3O_{12}]$ of the three oxides is almost the same whatever the nature of the A ion (Fig. 1): it is built up of corner-sharing octahedra and tetrahedra which form tunnels running along **b** where the A ions are located. Two tetrahedra out of three are linked to each other by sharing one corner, allowing the formulation $AMo_2O(PO_4)(P_2O_7)$ for these compounds. The equivalent Mo—O distances and the P—O distances (Table 3) are equal for the three members within the limits of 3σ.

The main difference concerns the position of the A ions in the tunnels as shown from a comparison of a projection of those structures along **b**. The rubidium ion (Fig. 1*b*) is only slightly displaced with respect to the thallium ion (Fig. 1*a*), in agreement with the very similar Tl—O and Rb—O distances (Table 3). This observation confirms the weak activity of the lone pair of Tl^+ in such a structure (Leclaire, Monier & Raveau, 1985*a*). The tendency of potassium to form shorter K—O distances induces a greater displacement of K^+ (Fig. 1*c*) with respect to Rb^+ and Tl^+. Two sets of positions are observed for K^+ which can be considered as mainly responsible for the doubling of the *a* parameter of $KMo_2P_3O_{12}$. One of the potassium ions, K(1), is only

Table 3. Mo—O *and* P—O *bond lengths and cation–oxygen distances* (Å) *in the three compounds*

	$TlMo_2P_3O_{12}$	$RbMo_2P_3O_{12}$		$KMo_2P_3O_{12}$
Mo—O(1)	1·855 (3)	1·862 (1)	Mo(1)—O(1)	1·847 (2)
			Mo(2)—O(2)	1·860 (2)
Mo—O(2)	2·02 (1)	2·013 (5)	Mo(1)—O(3)	2·036 (8)
			Mo(2)—O(4)	2·009 (7)
Mo—O(3)	2·05 (1)	2·072 (4)	Mo(1)—O(6)	2·065 (14)
			Mo(2)—O(5)	2·060 (11)
Mo—O(4)	2·02 (1)	2·026 (4)	Mo(1)—O(7)	2·026 (7)
			Mo(2)—O(8)	2·023 (8)
Mo—O(5)	2·03 (1)	2·024 (4)	Mo(1)—O(10)	2·048 (8)
			Mo(2)—O(9)	2·013 (7)
Mo—O(6)	2·04 (1)	2·014 (5)	Mo(1)—O(11)	2·010 (9)
			Mo(2)—O(12)	2·028 (8)
P(1)—O(2^{i})	1·53 (1)	1·517 (5)	P(1)—O(4^{vii})	1·533 (7)
P(1)—O(2^{ii})	1·53 (1)	1·517 (5)	P(1)—O(3^{viii})	1·531 (7)
P(1)—O(6)	1·51 (1)	1·523 (5)	P(1)—O(11^{vi})	1·539 (11)
P(1)—O(6^{iii})	1·51 (1)	1·523 (5)	P(1)—O(12^{vii})	1·500 (11)
P(2)—O(3^{iii})	1·54 (1)	1·516 (4)	P(2)—O(5^{vii})	1·528 (9)
			P(3)—O(6^{vii})	1·524 (11)
P(2)—O(4)	1·504 (9)	1·508 (4)	P(2)—O(7)	1·491 (8)
			P(3)—O(8)	1·515 (9)
P(2)—O(5^{iv})	1·49 (1)	1·503 (4)	P(2)—O(10^{xviii})	1·500 (7)
			P(3)—O(9^{xiv})	1·501 (7)
P(2)—O(7)	1·616 (8)	1·602 (8)	P(2)—O(13)	1·613 (6)
			P(3)—O(14)	1·607 (7)

A = Tl or Rb

	$TlMo_2P_3O_{12}$	$RbMo_2P_3O_{12}$	K—O	$KMo_3P_3O_{12}$
A—O(7^{v})	2·820 (17)	2·793 (7)	K(1)—O(13)	2·752 (13)
			K(2)—O(14^{viii})	2·701 (16)
A—O(2^{ii})	2·840 (12)	2·893 (5)	K(1)—O(3^{iv})	2·762 (7)
			K(2)—O(4)	2·782 (6)
A—O(2^{vi})	2·840 (12)	2·893 (5)	K(1)—O(3^{v})	2·762 (7)
			K(2)—O(4^{xiv})	2·783 (6)
A—O(6)	3·017 (12)	3·091 (5)	K(1)—O(12^{vi})	3·176 (11)
			K(2)—O(11^{vi})	2·917 (11)
A—O(6^{vii})	3·017 (12)	3·091 (5)	K(1)—O(12^{vii})	3·176 (11)
			K(2)—O(11^{xv})	2·917 (11)
A—O(3^{i})	3·227 (10)	3·191 (4)	K(1)—O(5)	3·181 (11)
			K(2)—O(6^{xvi})	3·123 (13)
A—O(3^{viii})	3·227 (10)	3·191 (4)	K(1)—O(5^{vii})	3·181 (11)
			K(2)—O(6^{xvii})	3·123 (13)
A—O(1^{ii})	3·286 (13)	3·273 (5)	K(1)—O(1^{viii})	3·292 (13)
			K(2)—O(2)	3·280 (14)

Symmetry operators: (i) $-x, -y, -z$; (ii) $-x, 0{\cdot}5+y, z$; (iii) $x, 0{\cdot}5-y, -z$; (iv) $1-x, 0{\cdot}5+y, z$; (v) $-x, y-0{\cdot}5, z$; (vi) $-x, 0{\cdot}5+y, 0{\cdot}5-z$; (vii) $x, y, 0{\cdot}5-z$; (viii) $-x, -y, 0{\cdot}5+z$; (ix) $x, 1-y, z$; (x) $x, 1-y, 0{\cdot}5-z$; (xi) $x, 1-y, 1-z$; (xii) $-x, 1-y, z-0{\cdot}5$; (xiii) $x, 1+y, z$; (xiv) $x, y, 1{\cdot}5-z$; (xv) $-x, 1-y, 0{\cdot}5+z$; (xvi) $x, 1+y, 1+z$; (xvii) $x, 1+y, 0{\cdot}5-z$; (xviii) $0{\cdot}5-x, 0{\cdot}5+y, z$; (xix) $0{\cdot}5-x, y-0{\cdot}5, z$.

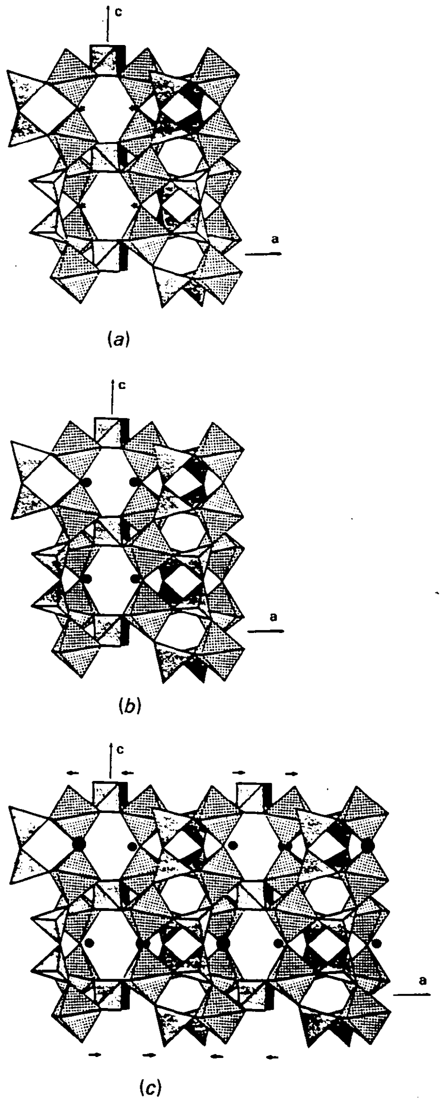

Fig. 1. Projection onto the *ac* plane of (*a*) $TlMo_2P_3O_{12}$, (*b*) $RbMo_2P_3O_{12}$, (*c*) $KMo_2P_3O_{12}$.

---

* Lists of structure factors and anisotropic thermal parameters have been deposited with the British Library Document Supply Centre as Supplementary Publication No. SUP 44192 (26 pp.). Copies may be obtained through The Executive Secretary, International Union of Crystallography, 5 Abbey Square, Chester CH1 2HU, England.

slightly displaced with respect to Tl^+ or Rb^+ (Fig. 1), whereas the second, K(2), is more displaced, especially along **a** in two opposite directions alternately (see arrows in Fig. 1*c*). In the three compounds the environment of the *A* ion remains rather similar: each *A* ion exhibits three short *A*—O distances (Table 3) corresponding approximately to the sum of the ionic radii (Shannon, 1976). However, the anisotropic displacement of K(2) means that it is characterized by a short K(2)—O(14) distance and two longer K(2)—O(4) distances, unlike K(1) which exhibits three equivalent K(1)—O distances, like rubidium and thallium.

The behaviour of the univalent *A* ions in the oxides $AMo_2P_3O_{12}$ is to be compared with that observed for the oxides $AMo_3P_6Si_2O_{25}$ (Leclaire, Borel, Grandin & Raveau, 1985) which are also characterized by a tunnel structure. In both compounds the size of the *A* ion does not influence the geometry of the host lattice which seems to be rather rigid owing to the presence of SiO_4 and PO_4 tetrahedra. However, the localization of the *A* ions is rather different in the two series of oxides: in $AMo_3P_6Si_2O_{25}$ the thermal agitation of the *A* ion increases drastically as its size decreases, whereas in $AMo_2P_3O_{12}$ the thermal agitation, although rather high ($B_{eq} \sim 3$ Å^2), remains constant, the *A* ion being slightly displaced as its size decreases in order to reach K—O distances compatible with the sum of the ionic radii.

References

International Tables for X-ray Crystallography (1974). Vol. IV. Birmingham: Kynoch Press. (Present distributor D. Reidel, Dordrecht.)

KIERKEGAARD, P. (1962). *Ark. Kemi*, **19**, 51–74.

LABBÉ, PH., GOREAUD, M., RAVEAU, B. & MONIER, J. C. (1978). *Acta Cryst.* B**34**, 1433–1438.

LECLAIRE, A., BOREL, M. M., GRANDIN, A. & RAVEAU, B. (1985). *Mater. Chem. Phys.* **12**, 537–543.

LECLAIRE, A., MONIER, J. C. & RAVEAU, B. (1984). *Acta Cryst.* B**40**, 180–185.

LECLAIRE, A., MONIER, J. C. & RAVEAU, B. (1985*a*). *J. Solid State Chem.* **59**, 301–305.

LECLAIRE, A., MONIER, J. C. & RAVEAU, B. (1985*b*). *Acta Cryst.* C**41**, 1719–1720.

MAGNÉLI, A. (1949*a*). *Ark. Kemi*, **1**, 213–221.

MAGNÉLI, A. (1949*b*). *Ark. Kemi*, **1**, 269–272.

MAGNÉLI, A. (1952). *Nature (London)*, **169**, 791–792.

MAGNÉLI, A. (1953). *Acta Chem. Scand.* **7**, 315–324.

MAGNÉLI, A. & BLOMBERG, B. (1951). *Acta Chem. Scand.* **5**, 372–378.

RAVEAU, B. (1986). *Proc. Ind. Acad. Sci. (Chem. Sci.)* **96**, 419–448.

SHANNON, R. D. (1976). *Acta Cryst.* A**32**, 751–767.

Acta Cryst. (1988). C**44**, 229–232

Structure of Hexaaquahydrogen Tetrachloroferrate(III) at 210 K by X-ray Diffraction

BY TORBJÖRN GUSTAFSSON

Institute of Chemistry, University of Uppsala, PO Box 531, *S*-751 21 *Uppsala, Sweden*

(*Received* 21 *April* 1987; *accepted* 5 *October* 1987)

Abstract. The structure of hexaaquahydrogen tetrachloroferrate(III), $HFeCl_4.6H_2O$, has been determined from single-crystal X-ray diffractometer data collected at 210 K. $[H_{13}O_6]^+.[FeCl_4]^-$, $M_r = 306{\cdot}76$, orthorhombic, *Pnma*, $a = 12{\cdot}470\,(2)$, $b = 15{\cdot}371\,(3)$, $c = 6{\cdot}286\,(1)$ Å, $V = 1204{\cdot}9\,(5)$ Å^3, $Z = 4$, $D_x = 1{\cdot}69\,(1)$ Mg m^{-3}, Mo $K\alpha$ radiation, $\lambda = 0{\cdot}71073$ Å, $\mu = 2{\cdot}14$ mm^{-1}, $F(000) = 620$. Refinement based on F^2 including 4781 reflexions gave a final $R(F)$ of 0·020. The structure consists of disordered layers of water–proton complexes interleaved with $FeCl_4^-$ ions. The $FeCl_4^-$ ions are almost regular tetrahedra, which are linked to form chains. The water–proton layers contain four-, five- and six-membered rings of water molecules.

Introduction. This work is part of a project concerned with the structure of hydrated protons. Earlier works describe the geometry of hydrated protons. It is shown that anion properties and water–proton ratios influence the formation of hydrated protons (Lundgren, 1974; Lundgren & Olovsson, 1976; Taesler, 1981). The presence of a highly charged metal ion in a structure can also influence the formation of hydrated protons, either by increasing the number of 'free' protons (Brunton & Johnsson, 1975) or by decreasing the number of water molecules that can take part in the formation of the hydrated proton (Gustafsson, Lundgren & Olovsson, 1977, 1980).

In the present compound, with its unusually large water–proton ratio and its medium-sized univalent anion, one would expect the formation of a large non-isolated water–proton complex.

Experimental. A spherical crystal of $HFeCl_4.6H_2O$ was grown using the technique described in a previous paper (Gustafsson, 1987), radius 0·15 mm, 210 K, cell

0108-2701/88/020229-04$03.00